Bull. Mater. Sci., Vol. 24, No. 6, December 2001, pp. 643–648. © Indian Academy of Sciences.

Effect of zirconium addition on the recrystallization behaviour of a commercial Al–Cu–Mg alloy

K T KASHYAP

Department of Mechanical Engineering, M.S. Ramaiah Institute of Technology, Bangalore 560 054, India

MS received 24 May 2001; revised 24 August 2001

Abstract. **It is well known that the second phase particles have an effect on recrystallization and grain growth behaviour of an alloy. Particularly the bimodal distribution of second phase particles has an effect which is opposite in sense where coarse second phase particles (> 1 μm) stimulate nucleation while fine particles exhibit Zener drag.**

In the literature, the effect of zirconium addition to aluminium alloys has been well documented in order to produce superplasticity by giving ultra fine grain size to the alloy. Addition of zirconium produces Al_3Zr particles which pin the grain boundaries during recrystallization and grain growth.

In the present work, zirconium was added to a commercial Al–Cu–Mg alloy and by heat treatment Al_3Zr particles were precipitated and after forging, the grain size was an order of magnitude lower than the alloy without zirconium.

Transmission electron microscopy was employed to characterize the second phase particles, i.e. Al_3Zr particles and found to be rod shaped and identified to be cubic ordered $L1_2$ phase with a lattice parameter of 0·408 nm. Further, it was observed that fine (100 nm) Al_3Zr particles promote only continuous recrystallization which is polygonization of subgrains and subgrain growth.

It was found that the fine dispersion of Al_3Zr particles inhibits both recrystallization and grain growth in the commercial Al–Cu–Mg alloy.

Keywords. **Al–Cu–Mg alloy; recrystallization; Al_3Zr particles; Zr addition.**

1. Introduction

It is well known that recrystallization behaviour of an alloy is altered by the presence of second phase particles. Coarse second phase particles (> 1 μm) stimulate recrystallization by a mechanism known as particle stimulated nucleation (PSN) as shown by Humphreys (1977). However, fine particles (< 1 μm) inhibit primary recrystallization and grain growth as described by Nes (1976). The drag exerted by second phase particles is known as Zener drag as quoted by Smith (1948). It is found by Doherty and Martin (1962) that as the spacing between second phase particles increases, grain size drops and time to 50% recrystallization drops. Doherty and Martin (1962) have also shown that as F_v/r is increased, nucleation rate increases and at a critical F_v/r, nucleation rate drops to low values. Precipitation during recrystallization alters the recrystallization behaviour which has been reviewed by Hornbogen and Koster (1978).

Importantly, a bimodal distribution of second phase particles affects the recrystallization behaviour in a peculiar way as described by Nes (1976). Coarse constituent particles stimulate nucleation of recrystallization whereas fine second phase particles inhibit recrystallization. This opposite effect of second phase particles in controlling recrystallization behaviour is important in commercial aluminium alloys.

The parameter which controls this behaviour is F_v/r, where F_v is the volume fraction of fine second phase particles and r, the average radius of the fine particles. Increasing F_v/r of fine particles increases the critical radius of the coarse particles to stimulate PSN as shown by Nes (1985).

Based on the models developed by Nes (1985), Wert and Austin (1985) and Nes and Hutchinson (1989), the main parameter which determines the final grain size after annealing an alloy which contains a volume fraction F_v of small particles of mean radius r is F_v/r. F_v/r affects the Zener drag given by

$$P_Z = \frac{3F_v g}{2r},$$

where P_Z is the Zener drag, g the surface energy of the high angle boundary, F_v the volume fraction of fine second phase particles, r the mean radius of second phase particles. F_v/r also affects the number of viable recrystallization nuclei given by

$$d_g = \frac{4g}{P_D - P_Z} = \frac{4g}{\frac{rGb^2}{2} - \frac{3F_v g}{2r}},$$

where d_g is the critical particle size for the growth of the viable nucleus, g the surface energy of the boundary, P_D the driving pressure, P_Z the Zener drag, r the dislocation density, G the shear modulus and b the burger's vector.

Finally F_v/r affects grain growth by

$$D_{lim} = \frac{4r}{3F_v}.$$

Grimes *et al* (1976), Watts *et al* (1976) and Matsuki *et al* (1976, 1977) have shown that zirconium addition to aluminium alloys makes them super plastic by stabilizing ultra fine grain size by the effect of fine Al_3Zr particles. Al_3Zr particles inhibit discontinuous recrystallization and promote only continuous recrystallization and fine particles also inhibit grain growth.

In the present work, zirconium was added to a commercial Al–Cu–Mg alloy to inhibit recrystallization and grain growth. The bimodal distribution of Al_3Zr and the constituent particles of Fe–Mn phase have been studied for their effects on recrystallization behaviour and grain growth behaviour after commercial processing. Detailed transmission electron microscopic characterization of Al_3Zr particles has also been carried out.

2. Experimental

The commercial aluminum alloy, V-65 was d.c. cast with zirconium addition of 0·16%Zr and without zirconium. Table 1 shows chemical composition of the alloys. The d.c. cast billet was homogenized at 490°C for 24 h and furnace cooled and then a low temperature treatment was given at 300°C for 48 h and air cooled. Electrical conductivity increased from 30% IACS in the cast state to 41% IACS after 300°C treatment indicating precipitation from the supersaturated d.c. cast ingot. The billets were deformed by the C-process and forged in a closed die forging equipment at 430°C.

Samples were sectioned and polished by conventional mechanical methods and etched in Keller's reagent. Samples were examined under optical microscope and scanning electron microscope (LEO 440). Samples were polished with Struers double jet polisher with 10% perchloric acid, balance methanol solution and thin foils were examined on a transmission electron microscope (JEOL 100KV microscope). Volume fractions and particle sizes of second phase particles were determined by image analysis.

3. Results and discussion

The d.c. cast billet (alloy V-65) which was homogenized and precipitated showed a conductivity increase from 30% IACS to 41% IACS from the as cast state to fully precipitated state, respectively.

Figure 1 shows the backscattered electron image of the alloy after low temperature treatment. The fine and coarse particles which look bright are Fe–Mn phase. Table 2 shows the SEM–EDX results of this phase. Image analysis was carried out and the volume fraction of these particles is found to be 0·05 with a mean radius of particles to be 0·37 μm. Al_3Zr particles are also present but it cannot be identified on the SEM or on the optical microscope.

Figures 2 and 3 show the microstructure of the alloy with 0·16% Zr at two different magnifications. The recrystallized grain size is of the order of 4–5 μm.

Figures 4 and 5 show the microstructure of the alloy without Zr at two different magnifications. The recrystallized grain size is of the order of 50–60 μm. All these microstructures were taken after homogenization, C-deformation and forging.

Figure 1. Backscattered electron image of the alloy after low temperature treatment.

Table 1. Chemical composition of V-65 alloys (in wt%).

	Cu	Mg	Si	Fe	Mn	Zr	Al
Alloy A	4·5	0·19	0·13	0·17	0·40	0·16	Bal
Alloy B	4·5	0·19	0·13	0·17	0·40	–	Bal

Table 2. SEM–EDX results of the Fe–Mn phase (at%).

Mn	Fe	Cu	Al
0·36	0·54	10·81	88·29

There is a dramatic reduction of grain size (4–5 μm) with Zr addition as compared to the alloy without Zr addition (50–60 μm). The Al_3Zr particles are not resolved on the SEM either in the secondary electron imaging or backscattered electron imaging. Therefore transmission electron microscopy of thin foils was carried out.

Figures 6 and 7 show the bright field TEM image of the precipitates. Figures 8 and 9 show the electron diffraction patterns. The rod shaped precipitates were identified to be Al_3Zr particles with a ordered $L1_2$ structure with a lattice parameter of 4·08 Å. The average particle size is found to be 100 nm. It is also observed from the bright field TEM images (figures 6 and 7) that the subgrain structure is pinned by rod shaped Al_3Zr particles. This means only continuous recrystallization is promoted by the fine dispersion of Al_3Zr particles.

This is the reason why a fine grain size is obtained by zirconium addition as shown in figures 2 and 3 at two different magnifications as opposed to figures 4 and 5 wherein without zirconium addition, the grain size is coarse in the alloy after the same treatment. The volume fraction of Al_3Zr particles was estimated from theoretical calculations as shown below.

Alloy composition (wt%)	Atomic weight
4·5 Cu	63·54
0·19 Mg	24·31
0·13 Si	28·09
0·17 Fe	55·85
0·40 Mn	54·94
0·16 Zr	91·22
94·51 Al	26·93

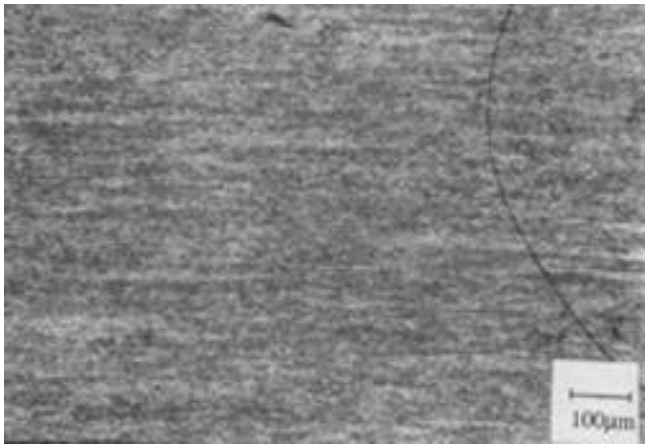

Figure 2. Microstructure of the alloy with Zr. Partially recrystallized (alloy A) showing fine grains.

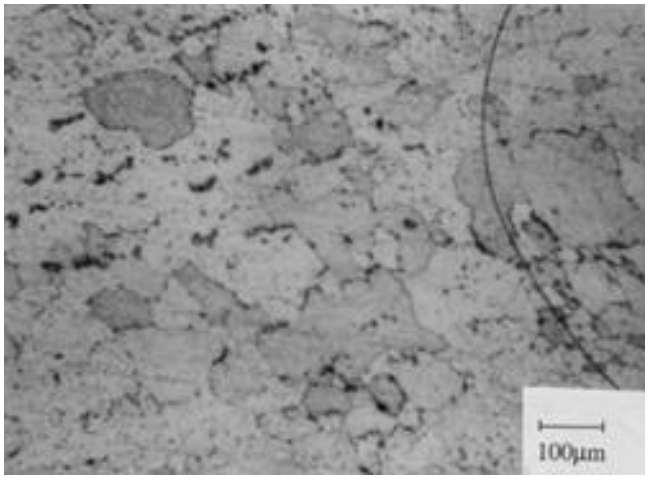

Figure 4. Microstructure of the alloy without Zr. Alloy B fully recrystallized followed by grain growth coarse grain size.

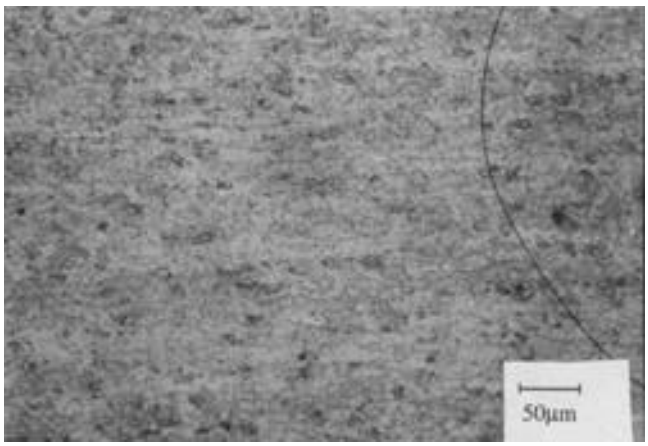

Figure 3. Microstructure of the alloy with Zr. Partially recrystallized (alloy A) at a higher magnification.

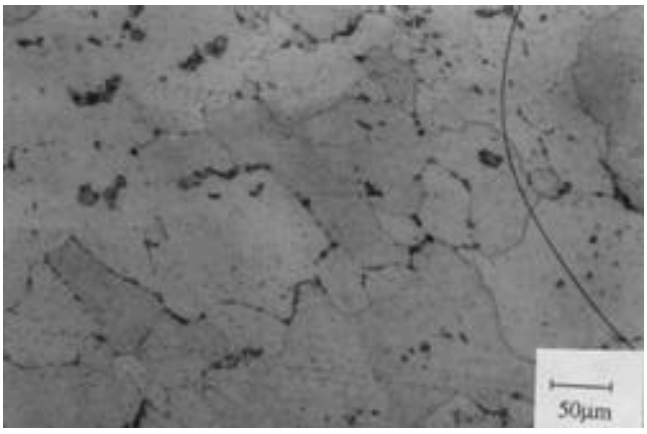

Figure 5. Microstructure of the alloy without Zr. Alloy B fully recrystallized followed by grain growth. Higher magnification photograph.

Atom fraction of zirconium,

$$= \frac{\frac{0\cdot16}{91\cdot22}}{\frac{4\cdot5}{63\cdot54}+\frac{0\cdot19}{24\cdot31}+\frac{0\cdot13}{28\cdot09}+\frac{0\cdot17}{55\cdot85}+\frac{0\cdot4}{54\cdot94}+\frac{0\cdot16}{91\cdot22}}$$

$= 0\cdot000486.$

At. fraction of Zr = 0·000486.

There are 3 atoms of Al and 1 atom of Zr in one molecule of Al_3Zr which means it has 4 atoms to 1 atom of zirconium. If the size of the unit cell of Al_3Zr is the same as that of aluminium which is to a very high degree of accuracy, then the atomic fraction of zirconium is the same as the volume fraction.

$F_v = 4 \times 0\cdot000486 = 0\cdot00194,$

$r = 100$ nm $= 0\cdot1$ μm.

However, there are bimodal dispersions (Fe–Mn and Al_3Zr phases) of second phase particles.

Fe–Mn phase, $F_v = 0\cdot05,$

$r = 0\cdot37$ μm.

Al_3Zr phase, $F_v = 0\cdot00194$

$r = 0\cdot1$ μms.

The zener drag is given by

$$P_Z = \frac{3F_v g}{2r}.$$

Total zener drag

$$P_{Z\,\text{total}} = \frac{3F_{v1}g}{2r_1} + \frac{3F_{v2}g}{2r_2}.$$

Equating driving force grain curvature to zener drag

$$\frac{2g}{D} = \frac{3F_{v1}g}{2r_1} + \frac{3F_{v2}g}{2r_2},$$

$$D_{\text{lim}} = \frac{2}{\frac{3F_{v1}g}{2r_1} + \frac{3F_{v2}g}{2r_2}},$$

$$D_{\text{lim}} = \frac{2}{\frac{3\times0\cdot05}{2\times0\cdot37} + \frac{3\times0\cdot00194}{2\times0\cdot1}},$$

$= 8\cdot6$ μms.

With a single dispersion i.e. without Al_3Zr

$$D_{\text{lim}} = \frac{4r}{3F_v} = \frac{4\times0\cdot37}{3\times0\cdot05} = 10\ \text{ìm}.$$

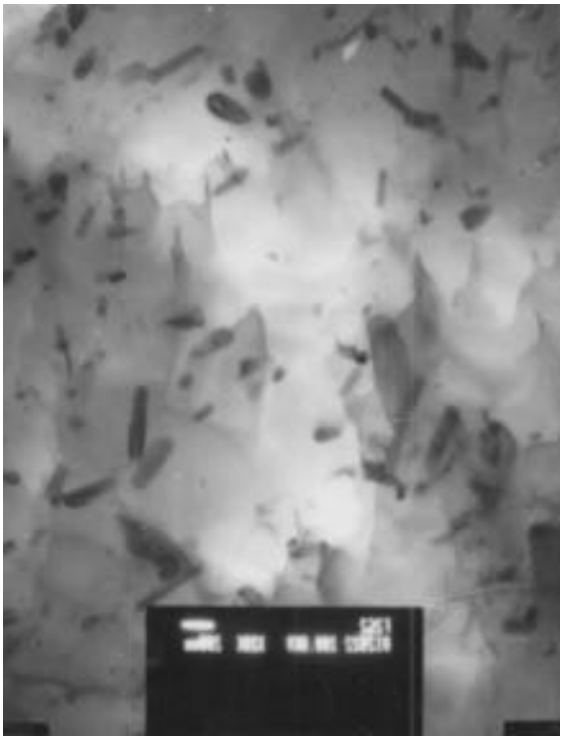

Figure 6. Bright field TEM image of the Al_3Zr particles which are rod shaped. Subgrain boundaries are pinned.

Figure 7. Bright field TEM image of the Al_3Zr particles (higher magnification). Subgrain boundaries are seen.

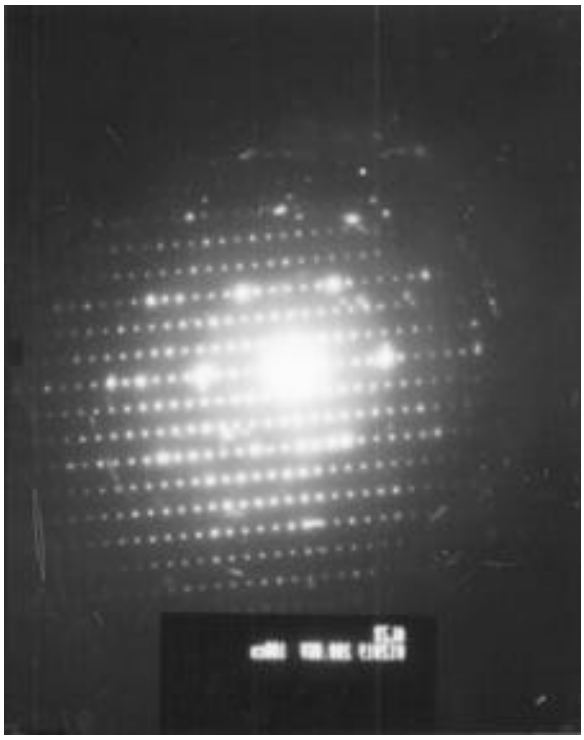

Figure 8. Electron diffraction pattern of Al_3Zr particles. Ordered $L1_2$ structure with $a = 0{\cdot}408$ nm.

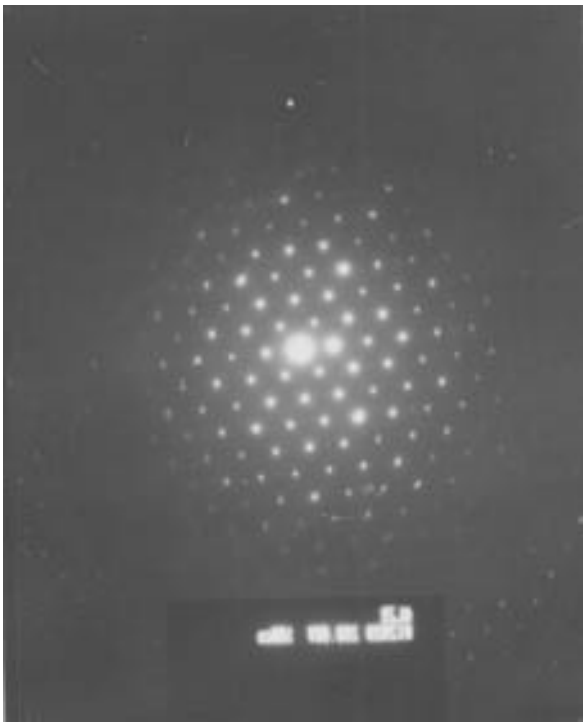

Figure 9. Electron diffraction pattern of Al_3Zr particles. Ordered $L1_2$ structure with $a = 0{\cdot}408$ nm.

In the homogenized and precipitated alloy, the recrystallized grain size is 4–5 μm which correlates with D_{lim} Zener (8·6 μm). The alloy without zirconium had a grain size of 50–60 μm. But this analysis ignores the fact that the Al_3Zr phase is coherent with the matrix and so should exert a larger drag than the incoherent phase. Since the volume fraction of Al_3Zr particles is low, the effect of Fe–Mn phase is predominant.

However, although the volume fraction of Al_3Zr particles in the microstructure is low, it has a pronounced effect on recrystallization as seen in figures 6 and 7 which show subgrains in the background which is pinned by rod shaped Al_3Zr particles.

Nucleation of recrystallization is associated with subgrain coalescence as shown by Doherty and Cahn (1972) by glide and climb of dislocations which form low angle boundaries adjacent to neighbouring high angle boundaries. Fine Al_3Zr particles inhibit this rearrangement of dislocations and also prevent migration of high angle boundaries. Thus nucleation of recrystallization is retarded. Only continuous recrystallization is promoted wherein polygonization and subgrain growth are favoured.

Finally, grain growth is also retarded by the fine dispersion of Al_3Zr particles. Therefore, the fine dispersion of Al_3Zr particles has an effect on primary recrystallization and grain growth following primary recrystallization.

This effect is consistent with the study of Watts *et al* (1976) where they added 0·5% Zr to Al–Cu alloy to achieve a very fine grain size to allow superplasticity at high temperature.

4. Conclusions

(I) TEM results show that Al_3Zr particles pin subgrain boundaries and promote continuous recrystallization.
(II) As a result of which the grain size after recrystallization has dropped to 5 μm from 60 μm after addition of zirconium to the alloy and giving it low temperature treatment.
(III) Fe–Mn phase is produced during d.c. casting as coarse (> 1 μm) particles as a result of solidification. These particles promote PSN. But the fine particles precipitated together with Al_3Zr exhibits Zener drag and controls recrystallization and grain growth.
(IV) Fine Al_3Zr and Fe–Mn particles control recrystallization and grain growth in this commercial Al–Cu–Mg alloy.

References

Doherty R D and Cahn R W 1972 *J. Less Common Metals* **28** 279

Doherty R D and Martin J W 1962 *J. Inst. Metals* **91** 332
Grimes R, Stowell M J and Watts B M 1976 *Met. Technol.* **3** 154
Hornbogen K and Koster U 1978 in *Recrystallization of metallic materials* (ed.) F Haaesner (Stuttgart, Germany: Riederer Verlag Gmbh)
Humphreys F J 1977 *Acta Metall.* **25** 1323
Matsuki K, Netani Y, Yamada M and Murakani Y 1976 *Met. Sci*. **10** 235
Matsuki K, Moriba H, Yamada M and Murakani Y 1977 *Met. Sci.* **11** 156
Nes E 1976 *Acta Metall*. **24** 391
Nes E 1985 *Proc. symp. on microstructural control during processing of aluminium alloys, New York*, p. 95
Nes E and Hutchinson W B 1989 *Proc. 10th int. Riso symp.* (ed.) Bilde Sorensen (Roskilde, Denmark: Riso National Laboratories) p. 233
Smith C S 1948 *Trans. Metall. Soc. AIME* **15** 175
Watts B M, Stowell M J, Baikie B L and Owen D G E 1976 *Met. Sci*. **10** 189, 198
Wert J A and Austin L K 1985 *Met. Trans.* **A19** 617